Shape Sensitivity Analysis and Optimization Using MSC/NASTRAN

R. J. Yang
Research Staff
Ford Motor Company

February 12, 1990

Abstract

Major software improvements have been made by MSC in the area of structural optimization. Grid point sensitivity is available in version 67 (alpha). This paper tests this capability by comparison with analytical solutions. Suggestions for further improvements are identified as well as recommendations for its use. The new capability has been integrated into an optimization system for component design. Several examples including a cantilever beam, a simplified engine connecting rod, a cantilever plate, and an upper suspension control arm are analyzed and optimized using this system.

1 Introduction

Grid point sensitivity is available in MSC/NASTRAN version 67 (alpha) [1]. This capability provides response sensitivity with respect to grid location. It can be integrated with an optimizer in an automated process for selecting the best design shape of automotive components.

The new capability is embedded in solution sequence 200. It can be applied in static, normal mode, and buckling analyses. This paper evaluates the sensitivity capability for equivalent static analysis only. Normal mode and buckling analysis are not considered here.

Two approaches for shape design sensitivity analysis are found in the literature. One is the well-known discrete approach and the other is the continuum approach. Detailed information for these two approaches is available in [2,3,4,5,6]. As the discrete approach is used in MSC/NASTRAN, a brief background for this approach is given in the following.

First the system of equations for static finite element formulation is written as:

$$\mathbf{K}\mathbf{u} = \mathbf{F} \tag{1}$$

where $\mathbf{K}$ is the stiffness matrix, $\mathbf{u}$ the displacement vector, and $\mathbf{F}$ the force vector. Differentiate (1) implicitly with respect to the design variable vector $\mathbf{b}$ and rearrange terms to

obtain

$$\mathbf{K}\frac{\partial \mathbf{u}}{\partial \mathbf{b}} = -\frac{\partial \mathbf{K}}{\partial \mathbf{b}}\mathbf{u} + \frac{d\mathbf{F}}{d\mathbf{b}} \tag{2}$$

The analytical displacement derivative $\partial \mathbf{u}/\partial \mathbf{b}$ is obtained by solving the same system of equations as in (1) with different force vectors in the right hand side, provided that analytical derivatives $\partial \mathbf{K}/\partial \mathbf{b}$ and $d\mathbf{F}/d\mathbf{b}$ are available.

As the analytical forms of $\partial \mathbf{K}/\partial \mathbf{b}$ and $d\mathbf{F}/d\mathbf{b}$ depend on the type of finite element used, and thus are difficult to obtain for a general purpose code, approximations for those two terms are often made. The grid point sensitvity in MSC/NASTRAN is obtained by the semi-analytical method. The semi-analytical approach approximates the stiffness and force derivatives by using the finite difference method. The stiffness matrix $\mathbf{K}$ is first computed for the base line design. A new stiffness matrix $\mathbf{K}'$ is then computed for each perturbed design variable. The ratio between the difference in stiffness ($\mathbf{K}'$ -$\mathbf{K}$) and the design variable change ($\mathbf{b}'$ -$\mathbf{b}$) is the approximate stiffness derivative. The same approach can be taken for force derivative calculation. After the approximation for stiffness and force is made, the displacement derivative is obtained by solving (2) using the original decomposed stiffness matrix.

Grid point sensitivity is applied to problems where the geometry is the design variable. More specifically, the grid point or a set of grid points which relates to a mathematical curve or surface is the design variable. In order to obtain $\mathbf{K}'$ and $\mathbf{F}'$, a new grid location $\mathbf{x}$ in the finite element model must first be provided. In MSC/NASTRAN 67 the following equation is used for updating the grid location:

$$\begin{pmatrix} x \\ y \\ z \end{pmatrix} = \begin{pmatrix} x \\ y \\ z \end{pmatrix}^0 + \sum_{k=1}^{n} b_k * coeffi * \begin{pmatrix} D - cosine\ x \\ D - cosine\ y \\ D - cosine\ z \end{pmatrix} + \begin{pmatrix} C_x \\ C_y \\ C_z \end{pmatrix} \tag{3}$$

or it can be rewritten as an index form as:

$$x_i = x_i^0 + Q_{ik}b_k + C_i,\ i = 1,3,\ k = 1,n \tag{4}$$

where n is the number of design variables, x_i are new coordinates, x_i^0 are old coordinates, C_i are constants and Q_{ik} are the "reduced basis vectors" which are defined as:

$$Q_{ik} = coeffi * \begin{pmatrix} D - cosine\ x \\ D - cosine\ y \\ D - cosine\ z \end{pmatrix}. \tag{5}$$

The reduced basis vectors are input through the bulk data card DVGRID. The input format resembles the bulk data card FORCE in MSC/NASTRAN. The fields CID, N1, N2, N3 describe the direction of the grid perturbation while the field $coeffi$ defines the magnitude of grid perturbation with respect to the unit value of design variable defined in DVID [7]. The constant term C_i is computed to make necessary adjustments so that x_i is equal to x_i^0 for the initial values of the design variable b_k supplied by the user. One important parameter

associated with DVGRID card is DELB which is specified on the optimization parameter card DOPTPRM. DELB defines the step size for finite differencing in the stiffness. Difference error may result in unacceptable sensitivities, when DELB is not properly selected.

It is noted that the reduced basis vectors in (4) are related to the "velocity" (**V**) which is often used in shape optimization literature. Differentiate (4) with respect to b_k to obtain

$$\frac{dx_i}{db_k} = Q_{ik}, \; i = 1,3, \; k = 1,n \tag{6}$$

It is clear that $\mathbf{V} = dx_i/db_k = Q_{ik}$.

The velocity can be a constant or variable. The constant velocity is applied to a small perturbation case in which the finite element mesh is only generated once and the mesh is updated by (4). In this case, remeshing efforts, which are essential in shape optimization, are reduced to a minimum. However, for a large geometry change the solution may be unreliable due to mesh distortion error in the finite element model. In general, the velocity or basis vector is a variable and depends on the mesh generator and the current mesh which is updated in each design iteration to reflect the design change. In this research, the finite element mesh is updated and the velocity or basis vector is recomputed for each design iteration.

This paper evaluates the grid point sensitivity capability in MSC/NASTRAN 67. Sensitivity results are compared with the analytical and/or finite difference solutions. The new capability is then integrated into an optimization system for component design. A cantilever beam, simplified engine connecting rod, cantilever plate, and an upper suspension control arm are analyzed and optimized using this system. Finally, discussions and suggestions for further improvements are summarized.

2 Optimization Procedure

The general structural optimization problem to be solved is: find the set of design variables **b** that will

$$\begin{aligned} \text{Minimize} \quad & f(\mathbf{b}, \mathbf{u}, \boldsymbol{\sigma}) \\ \text{Subject to:} \quad & G_j(\mathbf{b}, \mathbf{u}, \boldsymbol{\sigma}) \leq 0, \quad j = 1,m \\ & b_k^l \leq b_k \leq b_k^u, \quad k = 1,n \end{aligned} \tag{7}$$

where f and G are the objective function and constraints, respectively, and **b** is the vector of design variables. The total number of constraints is m, and b_k^l and b_k^u are lower and upper bounds on the n design variables, respectively. In this paper, the objective function is taken to be the component volume. Constraints considered here include displacement and stress. The constraints are normalized with respect to their critical value. For example, the stress constraints are typically of the form

$$G = \frac{\sigma}{\sigma_c} - 1 \leq 0 \tag{8}$$

where σ_c is the critical or allowable stress.

The grid point sensitivity capability is embedded in solution sequence 200. In this current version, the optimizer is not fully integrated into the program. In order to automate the design process, one has to extract the necessary data from MSC/NASTRAN output and postprocess the results. OUTPUT2 and OUTPUT4 commands are used to output table DSCMCOL and matrices DSCM2 and RSP1R for optimization. DSCMCOL is the correlation table between sensitivity matrix columns and the responses associated with these columns. DSCM2 is the sensitivity matrix and RSP1R the response matrix.

A system flow chart as shown in Fig. 1 is used for optimization. The modular flow chart is modified from [8]. It begins with the DESINF module which reads the design and optimization information data such as the constraints, design variables, and objective function and stores this data in the data base. This module is executed only once in the optimization process.

The GENERIC module reads the design parameters from the data base and provides the necessary finite element models for analysis and velocity (basis vector) calculation.

Module GEMTRY prepares the input data set for MSC/NASTRAN which includes a regular finite element model and a design model. The finite element model includes grid location, connectivity, material properties, loading, and boundary conditions. The design model includes design variables, constraints, the objective function, and some optimization parameters.

After the NASTRAN analysis is completed, the SENSTY module extracts table DSCMCOL and matrices DSCM2 and RSP1R and performs optimization. New design parameters resulting from the optimizer CONMIN [9] are then stored in the data base and can be read by the GENERIC module for the next iteration.

3 Numerical Examples

Due to limitations of the computer resource (MSC/NASTRAN 67 resides on VAX 8650), the sizes of the following examples were chosen to be relatively small. Two solid and two shell examples were tested in this section. For the solid component, the sensitivities were computed by three different methods:

- material derivative approach [10,2]
- MSC/NASTRAN 67 with DELB=.1%
- MSC/NASTRAN 67 with DELB= 1%

The material derivative approach computes the analytical sensitivity by postprocessing finite element results. The results for these three methods are then compared with the finite difference solutions. For the shell component, as the material derivative solution is still under development, a thin cantilever plate which has an analytical solution was first used to verify the MSC/NASTRAN sensitivity solution. Sensitivities for a suspension control arm

obtained by using MSC/NASTRAN and by using the finite difference method were compared and discussed.

The grid point sensitivity capability is integrated into an automatic modular system for component design (Fig. 1). In this optimization system, linear approximation for the objective and constraint functions is used during the line search process. All examples use a 50% move limit. The CONMIN program [9] which uses the feasible direction algorithm is employed as the optimizer. The optimization process is terminated when the change in objective function value is within .1% and the violation in constraint value is within 3%.

3.1 Cantilever Beam

A solid cantilever beam, shown in Fig. 2, was used as an example. Fixed dimensions, loading, constraints, and 3 design variables are shown in Fig. 2 . The left end of the beam is clamped and a distributed load of 10,000 N. is applied to the right face. The NASTRAN model of this beam contains 69 grid points and 5 20-noded HEXA elements. Young's modulus is 1.0×10^7 Mpa, Poisson's ratio is 0.3, and the allowable bending stress is 3000 MPa.

The upper and lower surfaces of the beam, parallel to the XZ plane, are to be varied. Three design variables were chosen as one-half of the height of the beam as shown in Fig. 2. A quadratic surface was fitted through the nodes controlled by the design variables.

The volume and normalized coordinate stress sensitivities in the X-direction for 3 different nodes were computed (Fig. 2). Sensitivity results and error percentage with respect to finite difference results for the nominal design variable vector $\mathbf{b} = [4., 4., 4.]$ were shown in Table 1. The finite difference results are the ratios between the difference in volume or stress (column 3 - column 1) and 1% design change. The sensitivities were computed by three different methods; material derivative approach [10,2], MSC/NASTRAN 67 with DELB= .1% and 1%, respectively.

It is observed, from Table 1, that the sensitivities for the material derivative approach (column 5) and finite difference method (column 4) have good agreement. The MSC/NASTRAN 67 results (column 7 and 9), for both DELB= .1% and 1%, do not agree well with the above two methods. However, if the largest sensitivity coefficients in column 4 are compared (highlighted), consistency is found in all three methods. The worst results are obtained by using MSC/NASTRAN 67 with DELB=1% (column 9), provided that the finite difference results (column 4) are correct.

The cantilever beam was optimized using both the material derivative approach and MSC/NASTRAN 67 with DELB=.1%. The initial design has a volume of 4000 mm^3 for the design variable vector $\mathbf{b} = [4., 4., 4.]$. Design histories for the volume and the maximum stress constraint are shown in Fig. 3. Initial and final design variables are listed Table 2. It is noted that both approaches converge in this case. However, it takes only 4 iterations to reach the optimum design for the material derivative approach as opposed to 10 iterations for MSC/NASTRAN 67. The inaccurate sensitivities obtained by MSC/NASTRAN 67 may contribute to the slow convergence.

(1) item	(2) D. V.*	(3) p. value	(4)[1] F.D.	(5)[2] DSA	(6)[3] error%	(7)[4] MSC	(8)[5] error%	(9)[6] MSC	(10)[7] error%
Volume	1(4.)	4007.2	**180**	**177**	1.7	100	44.4	100	44.4
(4000)	2(4.)	4025.6	**640**	**645**	**0.8**	**800**	**25.0**	**800**	**25.0**
(mm^3)	3(4.)	4007.2	**180**	**177**	1.7	100	44.4	100	44.4
$G^\dagger$@62	1(4.)	.62343	**-.789**	**-.772**	**2.2**	**-.850**	**7.7**	**-1.09**	**38.1**
(.65499)	2(4.)	.65400	**-.025**	**-.011**	-	-.320	-	-.547	-
	3(4.)	.65510	**.003**	**.002**	-	.273	-	.051	-
$G^\dagger$@57	1(4.)	.23400	**-.291**	**-.292**	0.3	-.626	115.	-.839	188.
(.24563)	2(4.)	.22977	**-.397**	**-.407**	**2.5**	**-.630**	**58.7**	**-.836**	**111.**
	3(4.)	.24853	**.073**	**.074**	-	.567	-	.369	-
$G^\dagger$@52	1(4.)	-.05967	**-.053**	**-.055**	3.8	-.457	862.	-.696	1213
(-.05753)	2(4.)	-.07553	**-.450**	**-.447**	**0.7**	**-.494**	**9.8**	**-.670**	**48.9**
	3(4.)	-.05607	**.037**	**.033**	-	.409	-	.212	-

* design variable and value
† $G = \sigma_x/\sigma_c$ -1
[1] (4)=((3)-(1))/.01 b_i
[2] material derivative approach
[3] (6)=| 1- | (5)/(4) || x 100 %
[4] MSC/NASTRAN(67) (DELB=0.001)
[5] (8)=| 1- | (7)/(4) || x 100 %
[6] MSC/NASTRAN(67) (DELB=0.01)
[7] (10)=| 1- | (9)/(4) || x 100 %

Table 1: Sensitivity Comparison for Cantilever Beam

design variable	initial	final[1]	final[2]	lower bound	upper bound
1	4.	5.043	5.179	0.2	50.
2	4.	3.646	3.589	0.2	50.
3	4.	1.528	1.708	0.2	50.

[1] material derivative approach
[2] MSC/NASTRAN(67)

Table 2: Design Variables (in mm) for Cantilever Beam

3.2 Idealized Engine Connecting Rod

A simplified engine connecting rod was used as the second example. This example exists in the open literature [11] and is intended only to demonstrate the use of grid sensitivity capability from MSC/NASTRAN 67.

The right hole of the connecting rod which mates with the piston pin is fixed to eliminate rigid body motion. An arbitrarily selected pressure of 3000 MPa is applied to the left hole, distributed from 0 to 90 degrees, to simulate the firing forces. An octahedral shear stress constraint was imposed at each node in the finite element model of the connecting rod. The critical yield stress used for analysis was chosen as 3000 MPa. Young's modulus is 1.0×10^7 MPa and Poisson's ratio is 0.3. Note that the numerical data selected for this example are not necessarily realistic.

Using symmetric conditions, only a quarter of the structure needs to be analyzed. The generic model and design parameters are shown in Fig. 4. In this model, 8 design variables are chosen; 5 parameters define the shape of the shank and neck regions, 2 are the outer radii of the right and left holes, and 1 parameter defines the height of the web. The finite element model, as shown in Fig. 5, contains 105 solid elements, 928 nodal points, and 2126 degrees-of-freedom.

The volume and normalized octahedral shear stress sensitivities for 2 different nodes were computed (Fig. 5). The sensitivity results and error percentage with respect to finite difference sensitivities were shown in Table 3. The sensitivities were computed by three different methods: material derivative approach [10,2], MSC/NASTRAN 67 with DELB= .1% and 1%, respectively.

Table 3 summarizes different results. The finite difference results (column 4) were evaluated only for those which have relatively large magnitudes (column 5). It is noted that the sensitivities do not agree well between the different approaches, except for the largest sensitivity coefficient (highlighted). The material derivative approach gives the closest set of coefficients (column 5) compared with those obtained by the finite difference solutions (column 4). The worst results are again obtained by using MSC/NASTRAN 67 with DELB=1% (column 9). Poor results for sensitivities may result from the difference error due to small perturbations.

The connecting rod was optimized using both the material derivative approach and MSC/NASTRAN 67 with DELB=1%. Design histories for the volume and the maximum stress constraint are shown in Fig. 6. Initial and final design variables are listed on Table 4. It is observed that both approaches converge, however, to different solutions (Table 4). It takes 4 and 7 iterations to converge for the material derivative approach and for MSC/NASTRAN 67, respectively. The more quickly converging results for the material derivative approach may suggest that more accurate sensitivities are provided in this case.

3.3 Cantilever Plate

A simple cantilever plate subjected to a uniformly distributed load at the end was used as the third example. The geometry, material properties, and loads are shown in Fig. 7.

(1) item	(2) D. V.*	(3) p. value	(4)[1] F.D.	(5)[2] DSA	(6)[3] error%	(7)[4] MSC	(8)[5] error%	(9)[6] MSC	(10)[7] error%
Volume	1(5.478)	4566.100	63.6	56.2	11.7	10.9	82.9	10.5	83.5
(4562.519)	2(3.185)	-	-	242	-	318	-	318	-
(mm^3)	3(1.983)	-	-	105	-	39.3	-	39.3	-
	4(1.501)	-	-	177	-	232	-	232	-
	5(1.636)	-	-	44.9	-	18.3	-	18.1	-
	6(3.408)	4567.531	147	143	2.7	132	10.2	132	10.2
	7(24.00)	4748.140	**773**	**784**	**1.4**	**778**	**.6**	**780**	**.9**
	8(13.30)	-	-	517	-	500	-	502	-
$G^\dagger$@53	1(5.478)	3.86131	-.139	.602	-	-.055	-	-.134	-
(3.86897)	2(3.185)	-	-	.026	-	.120	-	.123	-
	3(1.983)	-	-	-.006	-	-.119	-	-.117	-
	4(1.501)	-	-	.000	-	.000	-	.000	-
	5(1.636)	-	-	.000	-	.000	-	.000	-
	6(3.408)	3.86386	-.150	.643	-	-.076	-	-.126	-
	7(24.00)	2.93543	**-3.89**	**- 5.43**	**39.5**	**-10.9**	**180**	**28.0**	**620**
	8(13.30)	-	-	.000	-	.000	-	.000	-
$G^\dagger$@118	1(5.478)	1.60191	.019	.205	-	.254	-	.200	-
(1.60088)	2(3.185)	-	-	-.010	-	-.038	-	-.038	-
	3(1.983)	-	-	.002	-	.037	-	.037	-
	4(1.501)	-	-	.000	-	.000	-	.000	-
	5(1.636)	-	-	.000	-	.000	-	.000	-
	6(3.408)	1.60081	-.002	.216	-	.257	-	.224	-
	7(24.00)	1.11861	**-2.01**	**-2.98**	**48.3**	**-8.52**	**324**	**22.2**	**1004**
	8(13.30)	-	-	.000	-	.000	-	.000	-

* design variable and value

† $G = \tau_o/\tau_c$ -1

[1] (4)=((3)-(1))/.01 b_i

[2] material derivative approach

[3] (6)=| 1- | (5)/(4) || x 100 %

[4] MSC/NASTRAN(67) (DELB=0.001)

[5] (8)=| 1- | (7)/(4) || x 100 %

[6] MSC/NASTRAN(67) (DELB=0.01)

[7] (10)=| 1- | (9)/(4) || x 100 %

Table 3: Sensitivity Comparison for Connecting Rod

design variable	initial	final[1]	final[2]	lower bound	upper bound
1	5.478	7.286	3.413	0.1	100.
2	3.185	1.829	2.176	0.1	100.
3	1.983	1.290	0.581	0.1	100.
4	1.501	0.793	0.486	0.1	100.
5	1.636	1.234	0.731	0.1	100.
6	3.408	4.128	5.564	0.1	100.
7	24.00	26.913	27.257	24.0	100.
8	13.30	13.30	13.30	13.3	100.

[1] material derivative approach
[2] MSC/NASTRAN(67)

Table 4: Design Variables (in *mm*) for Connecting Rod

Young's modulus is 1.0×10^7 MPa and Poisson's ratio is 0.3. The design variables for this plate are: thickness, width, and length. The vertical displacement at point A was chosen as a check point for sensitivity accuracy. Two CQUAD4 elements and 6 grids were used in this example.

As the thickness is small compared to the length of the plate, the analytical solution for classical beam theory can be used. The vertical displacement at A is 0.045568 mm and 0.048 mm, respectively, from MSC/NASTRAN 67 and the classical beam theory. This is 5.1% error in displacement.

The sensitivity results are listed in Table 5. It is found that the solutions from MSC/NASTRAN are within 5% of the exact solutions for all design variables.

3.4 Control Arm

An automotive upper suspension control arm which is modeled as shell elements was chosen as the fourth example [12]. The design model consists of 7 design variables as shown in Fig. 8. The first design variable is thickness which is commonly considered as a sizing variable, whereas the rest are shape design variables which define the geometry of the control arm.

The NASTRAN finite element model, shown in Fig. 9, contains 197 grid points and 152 QUAD4 elements. Fixed boundary conditions are applied at the two left holes and a total load of 140 lb is uniformly applied to the right hole vertically. Young's modulus is 2.9×10^7 psi, Poisson's ratio is 0.32, and the allowable shear stress is 1000 psi.

The volume and maximum shear stress sensitivities in three elements were computed (Fig. 9). Sensitivity results and error percentage with respect to finite difference results were shown in Table 6. The sensitivities were computed by MSC/NASTRAN 67 with DELB=.1% and 1%. The solution for the material derivative approach is not available in this case.

(1) item	(2) D.V.*	(3)[1] DSA	(4)[2] DSA	(5)[3] error %
thichness	1(1.)	-1.44 x 10^{-1}	-1.3685 x 10^{-1}	4.96
width	2(10.)	-4.8 x 10^{-3}	-4.6171 x 10^{-3}	3.81
length	3(10.)	7.2 x 10^{-3}	6.7908 x 10^{-3}	5.68

* design variable and value (mm)
[1] Classical beam theory
[2] MSC/NASTRAN(67)
[3] (5)=| 1- | (4)/(3) || x 100 %

Table 5: Sensitivity Comparison for Simple Plate

It is observed that the volume sensitivities have good agreement, while the stress sensitivities are very poor and inconsistent except for the thickness design variable (highlighted). In general, results for DELB=1% are worse than those of DELB=.1%. The poor sensitivities may result from small changes in stress quantities with respect to shape design change.

The control arm was optimized using MSC/NASTRAN 67 with DELB=.1%. Design histories for the volume and the maximum stress constraint are shown in Fig. 10. Initial and final design variables are listed in Table 7. It is shown that the convergent results are achieved in 7 iterations.

It is interesting to see optimization results for shape design variables only, as the sensitivity comparison is poor. Let the thickness variable (b_1) be kept fixed and only the shape variables allowed to vary. The iteration results for this case are shown in Fig. 10. It is observed that the volume and maximum shear stress both increase in 5 iterations, as the design variable reaches either upper or lower bound (table 7). This indicates that convergence is not achieved, as the design is not improved in this case. Another numerical experiment in which the critical stress is increased from 1000 psi to 1500 psi is also performed for shape design variables. In this case the initial design starts from the region where it is close to the feasible design. Fig. 10 shows that the convergence is achieved slowly.

4 Discussion and conclusions

During this study, several problems in MSC/NASTRAN were encountered. Most of them are inconsistency problems and should be easy to fix. They are summarized as follows:

- In this version tested, MSC/NASTRAN only provides response sensitivities. The constraint sensitivities have to be evaluated by using the response sensitivity, despite the fact that constraint commands are described in the User's Manual.

(1) item	(2) D. V.*	(3) p. value	(4)[1] F.D.	(5)[2] MSC	(6)[3] error%	(7)[4] MSC	(8)[5] error%
Volume	1(.2)	225.5450	**1250**	**1117**	**10.6**	**1117**	**10.6**
(223.3118)	2(3.)	223.4991	6.24	6.23	.2	6.23	.2
(in^3)	3(7.)	223.9945	9.75	10.6	8.7	10.6	8.7
	4(10.)	223.9845	6.73	4.43	34.2	4.4	34.6
	5(8.)	224.1297	**10.2**	**11.9**	**16.7**	**11.9**	16.7
	6(5.)	223.5945	5.65	7.96	40.9	7.93	40.4
	7(3.)	223.5776	8.86	12.3	38.8	12.3	38.8
$G^\dagger$@84	1(.2)	.43903	**-14.2**	**-14.5**	**2.1**	**-14.8**	**4.2**
(.46742)	2(3.)	.46744	.001	-.034	-	-.287	-
	3(7.)	.46735	-.001	-.005	-	-.088	-
	4(10.)	.46742	.000	-.006	-	-.034	-
	5(8.)	.47001	.032	-.106	-	-1.08	-
	6(5.)	.46728	-.003	-.044	-	-.294	-
	7(3.)	.46436	**-.102**	**-.228**	-	**-1.16**	-
$G^\dagger$@77	1(.2)	.38174	**-13.4**	**-13.7**	**2.2**	**-14.0**	**4.5**
(.40861)	2(3.)	.40861	.000	-.033	-	-.259	-
	3(7.)	.40855	-.001	-.004	-	-.073	-
	4(10.)	.40860	-.000	-.005	-	-.029	-
	5(8.)	.41672	**.101**	**-.121**	-	**-1.16**	-
	6(5.)	.40832	-.006	-.043	-	-.241	-
	7(3.)	.40708	-.051	-.109	-	-.572	-
$G^\dagger$@77	1(.2)	-.18843	**-7.83**	**-7.97**	**1.8**	**-8.18**	**4.5**
(-.17277)	2(3.)	-.17277	.000	-.0003	-	-.199	-
	3(7.)	-.17287	-.001	-.006	-	-.119	-
	4(10.)	-.17278	.000	-.008	-	-.046	-
	5(8.)	-.17246	.004	.0003	-	-.612	-
	6(5.)	-.17294	-.003	-.059	-	-.458	-
	7(3.)	-.17674	**-.132**	**-.209**	**58.3**	**-.903**	**584**

* design variable and value

† $G = \tau_{max}/\tau_c$-1

[1] (4)=((3)-(1))/.01 b_i

[2] MSC/NASTRAN(67) (DELB=0.001)

[3] (6)=| 1- | (5)/(4) || x 100 %

[4] MSC/NASTRAN(67) (DELB=0.01)

[5] (8)=| 1- | (7)/(4) || x 100 %

Table 6: Sensitivity Comparison for Control Arm

design variable	initial	final[1]	final[2]	final[3]	lower bound	upper bound
1	0.2	.242	0.2	0.2	.05	1.
2	3.	2.97	2.5	2.5	2.5	4.
3	7.	6.	8.	6.	6.	8.
4	10.	9.	12.	9.	9.	12.
5	8.	7.57	10.	4.968	4.	10.
6	5.	5.049	6.	4.274	4.	6.
7	3.	3.	4.	2.	2.	4.

[1] all variables
[2] shape variables, $\tau_c = 1000psi$
[3] shape variables, $\tau_c = 1500psi$

Table 7: Design Variables (in *in*) for Control Arm

- The item code which must be specified in the DRESP1 card for different response quantities is not consistent with the output file. For example, for solid elements, only octahedral shear stress sensitivity can be obtained, although von Mises stress is printed in the output file. For plate and shell elements, only maximum shear stress sensitivity is obtained, while the von Mises stress is printed in the output file.

- Sensitivities in the output file and data block are not consistent. The sensitivities in the output file are normalized with respect to the design variable, whereas they are not normalized in the data blocks extracted using OUTPUT2 and OUTPUT4.

- Input for the velocity or reduced basis vector through the DVGRID card is inconvenient for component design problems. In most automotive components, the interior grid locations as well as the exterior vary due to the design change. The large number of DVGRID cards are magnified by a large number of design variables. A matrix input capability and a CAD interface are required to alleviate the situation.

Further conclusions and findings are summarized as follows:

- The step size parameter DELB seems to be overly responsive to the sensitivity coefficients obtained by MSC/NASTRAN. In most cases, DELB =.1% seems to give better results. In the control arm example, both DELB=.1% and 1% apparently are insufficient to give accurate shape sensitivities for elemental maximum shear stress. In general, selecting an appropriate step size DELB is difficult. A large DELB may result in a large truncation error, while a small DELB may produce a large round-off error. It is suggested that the central difference method should be used for computing the stiffness derivative [13] or an error indicator should be provided for the user's information [14].

- In the solid component case, the sensitivities for the material derivative approach have good agreement with the finite difference solution. It is apparent that in the cantilever beam and connecting rod examples smaller numbers of iterations are required for convergence. More rapid convergence is achieved because analytical sensitivities are obtained in this case. In general, it is suggested to use analytical sensitivities whenever available.

- For the shell component, a simple cantilever plate demonstrated that the displacement sensitivity has good agreement with the analytical solution for sizing and shape design variables. The control arm example showed that good agreement was only obtained for the sizing design variable (thickness).

Aside from the aforementioned problems, the MSC/NASTRAN grid point sensitivity capability provides a valuable tool for the analyst.

5 Acknowledgement

The author wish to express appreciation to A. Lee for creating the generic control arm model.

References

[1] G. K. Nagendra and D. V. Wallerstein. Grid sensitivity capability for large scale structures. In *Second NASA/Air Force symposium on recent experiences in multidisciplinary analysis and optimization*, Hampton, Virginia, September 1988.

[2] E. J. Haug, K. K. Choi, and V. Komkov. *Design Sensitivity Analysis of Structural Systems.* Academic Press, 1986.

[3] J. A. Bennett and M. E. Botkin, editors. *The Optimum Shape: Automated Structural Design.* Plenum Press, New York, 1986.

[4] R. J. Yang and M. E. Botkin. Comparison between the variational and implicit differentiation approaches to shape design sensitivities. *AIAA Journal*, 24(6):1027–1032, 1986.

[5] R. J. Yang and M. E. Botkin. Accuracy of the domain material derivative approach to shape design sensitivities. *AIAA Journal*, 25(12):1606–1610, 1987.

[6] R. T. Haftka and R. V. Grandhi. Structural shape optimization - a survey. *Computer Methods in Applied Mechanics and Engineering*, 57:91–106, 1986.

[7] H. Miura. *Handbook for Structural optimization.* The MacNeal-Schwendler Corporation, Los Angeles, California, 1988.

[8] R. J. Yang, D. L. Dewhirst, J. E. Allison, and A. Lee. *Shape Optimization of Connecting Rod Pin End Using A Generic Model.* SR-89-115, FORD, 1989.

[9] G. N. Vanderplaats. *CONMIN - A fortran program for constrained function minimization user's manual.* TM X 62 282, NASA, 1973.

[10] R. J. Yang. A three-dimensional shape optimization system - SHOP3D. *Computers and Structures*, 31(6):881–890, 1989.

[11] R. J. Yang and M. E. Botkin. A modular approach for three-dimensional shape optimization. *AIAA Journal*, 25(3):492–497, 1987.

[12] M. E. Botkin and M. J. Fiedler. Graphics assisted design modeling for 2-d shape optimization. In *Proceedings of VII International Vehicle Structural Mechanics Conference*, Detroit, Michigan, 1988.

[13] P. A. Fenyes and R. V. Lust. Error analysis for semi-analytic displacement derivatives with respect to shape and size variables. In *Proceedings of 30th AIAA SDM Conference*, Mobile, Alabama, 1989.

[14] B. Barthelemy, C. Chon, and R. Haftka. Accuracy problems associated with semi-analytical derivatives of static response. *Finite Elements in Analysis and Design*, 4:249–265, 1988.

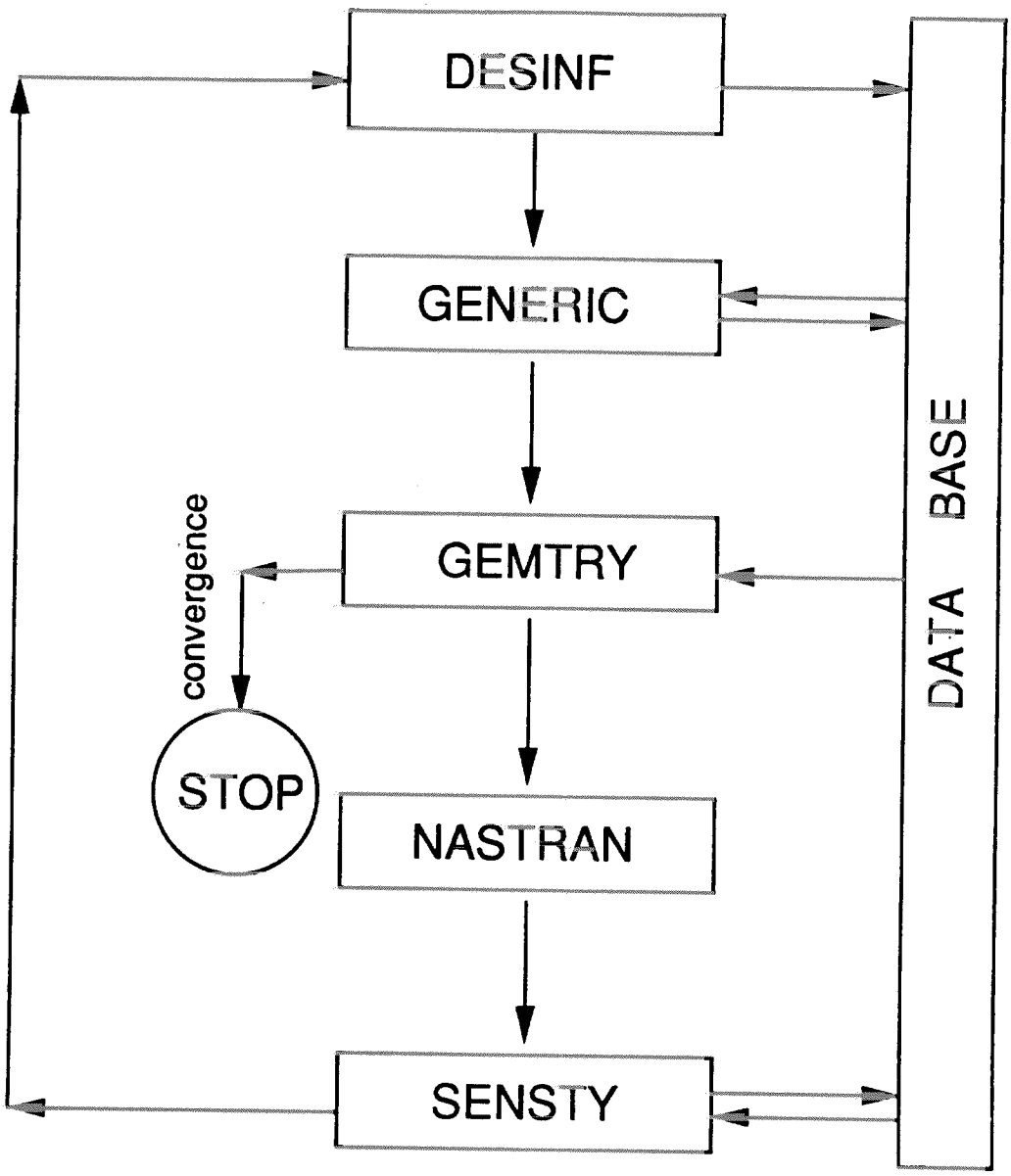

Figure 1: Modular System Flow Chart

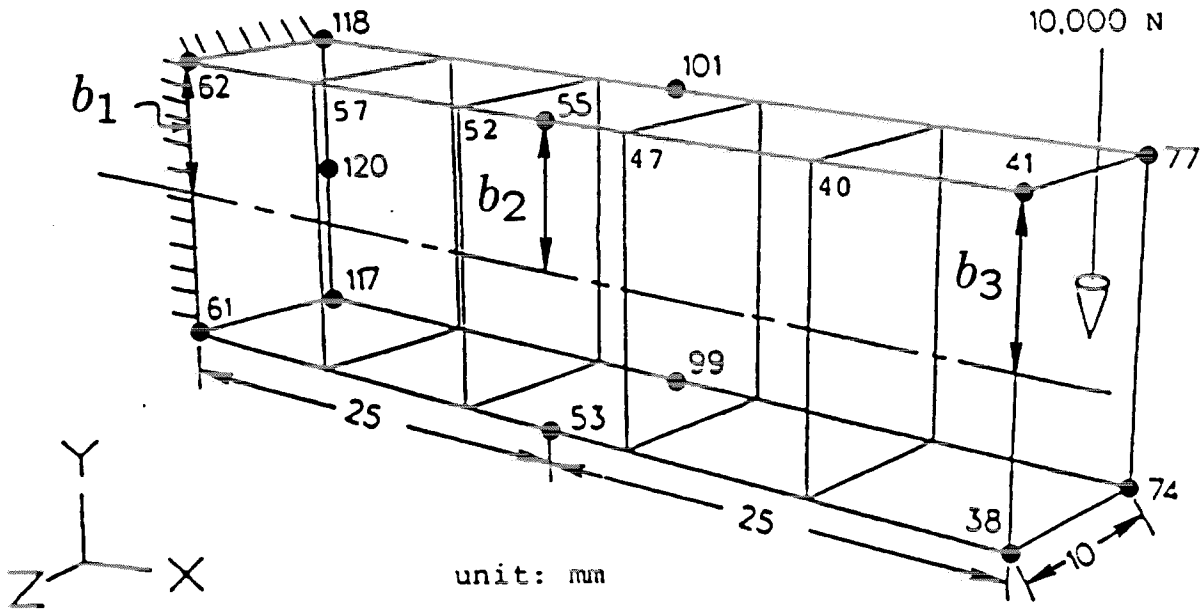

Figure 2: Finite Element and Design Model of Cantilever Beam

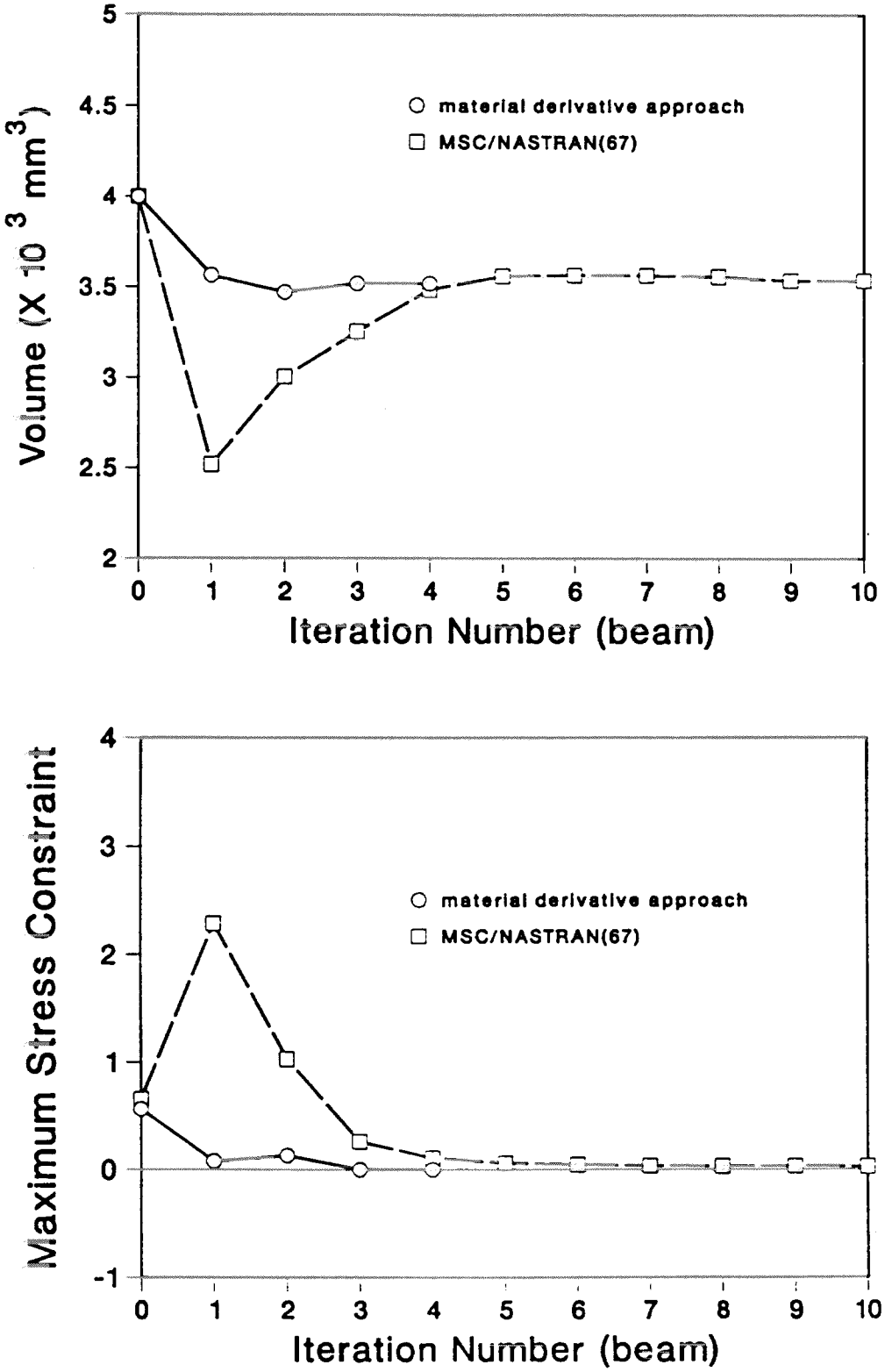

Figure 3: Design Histories of Cantilever Beam

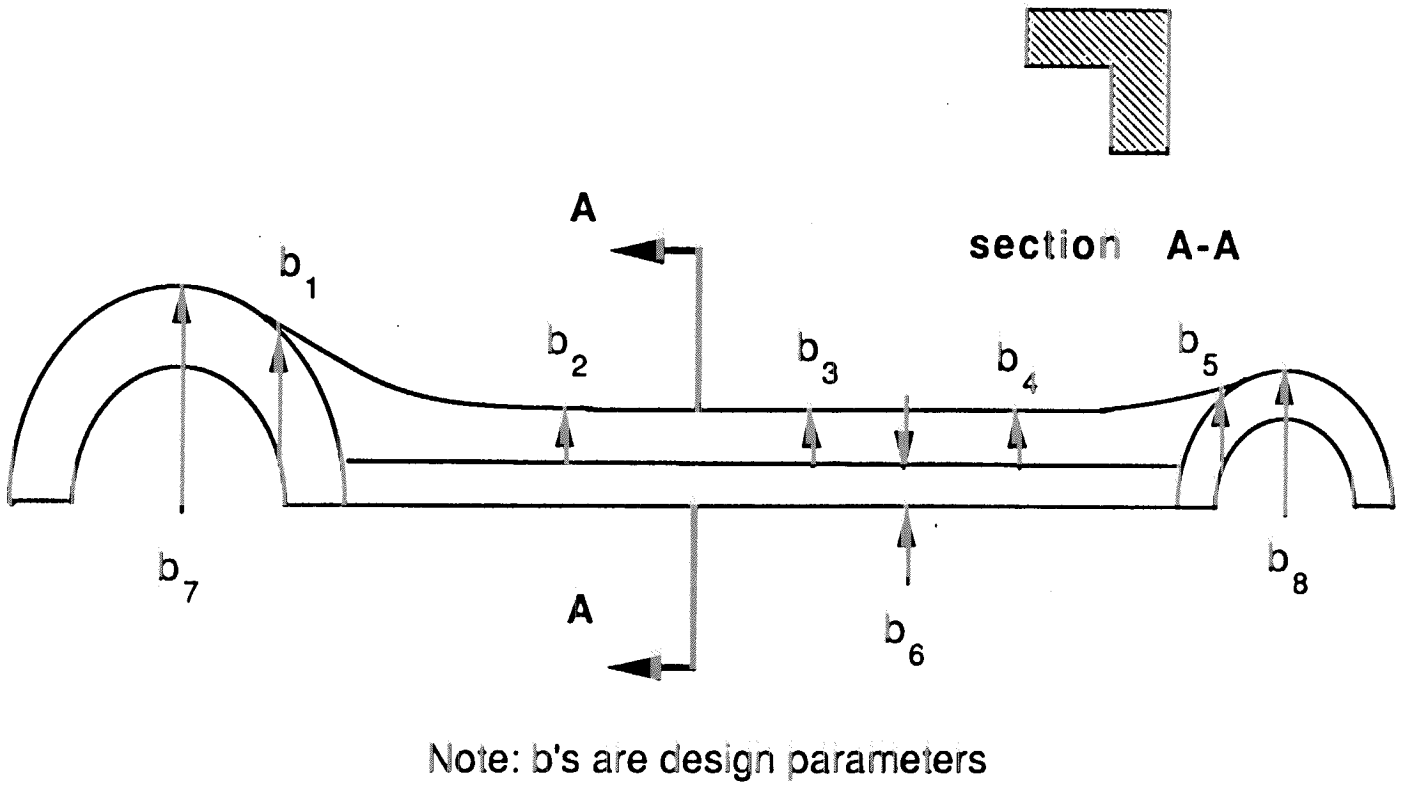

Figure 4: Design Model of Connecting Rod

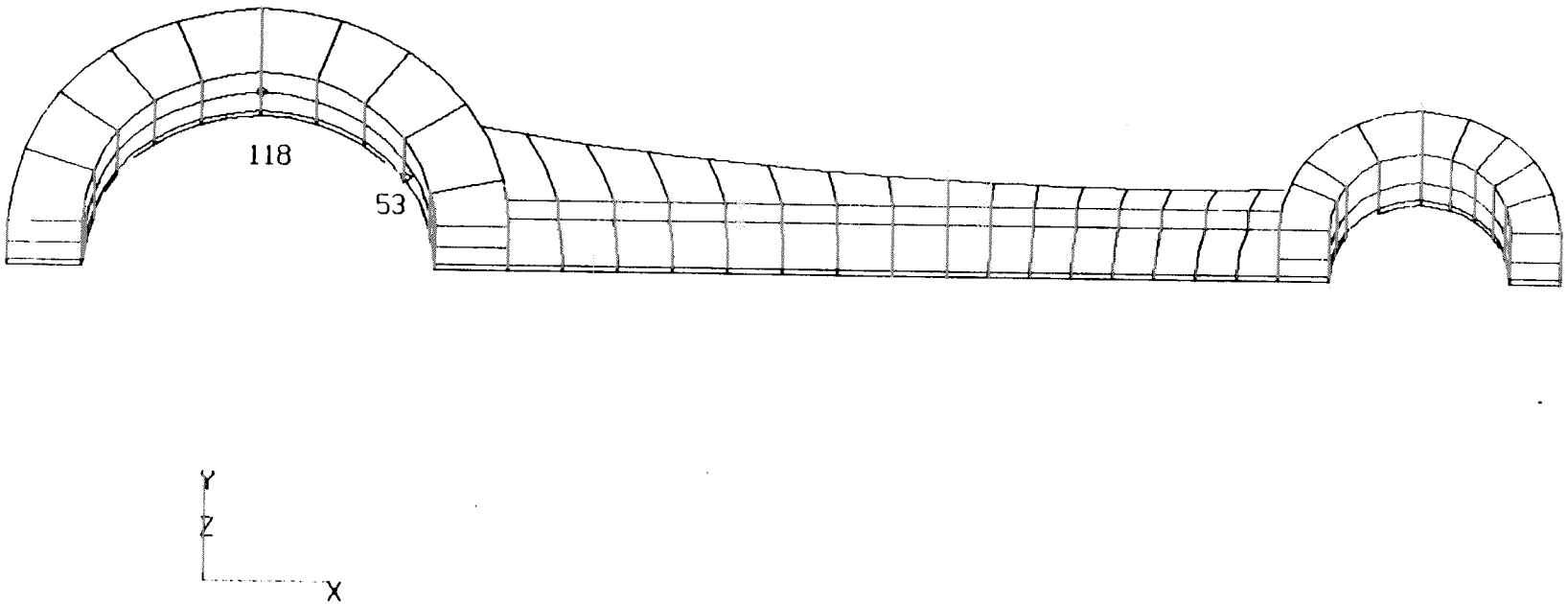

FIGURE 5: FINITE ELEMENT MESH OF CONNECTING ROD

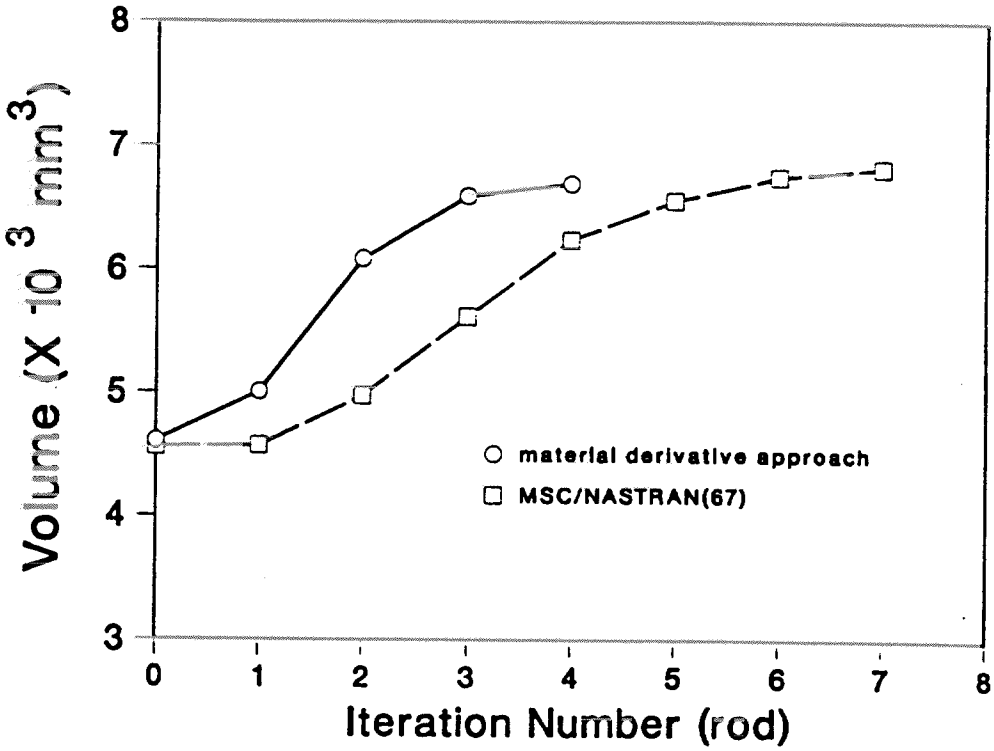

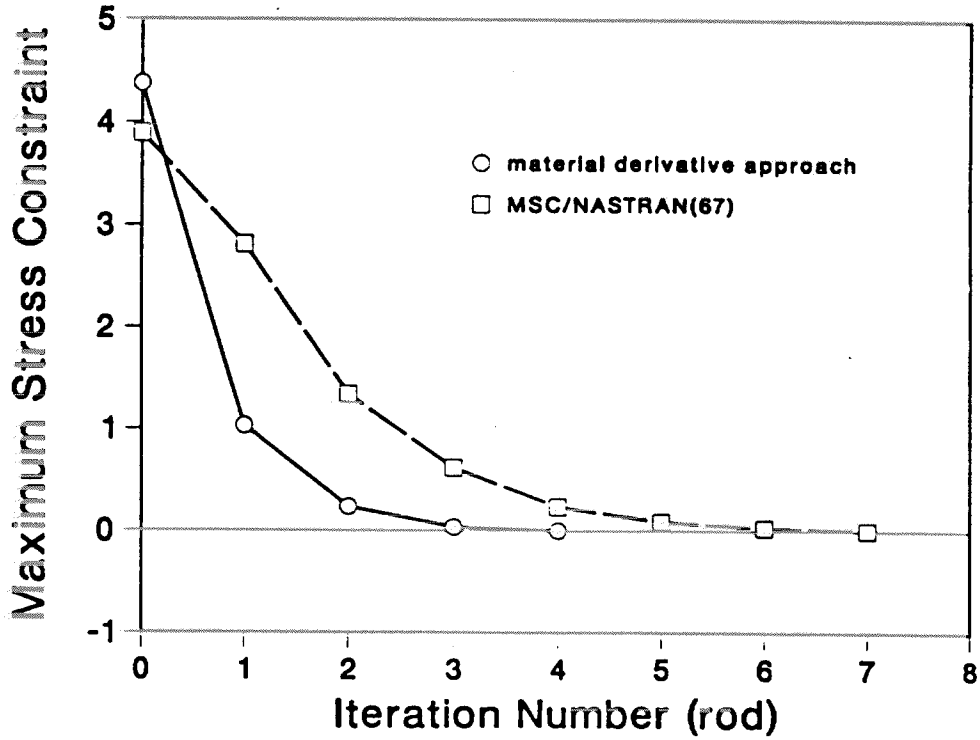

Figure 6: Design Histories of Connecting Rod

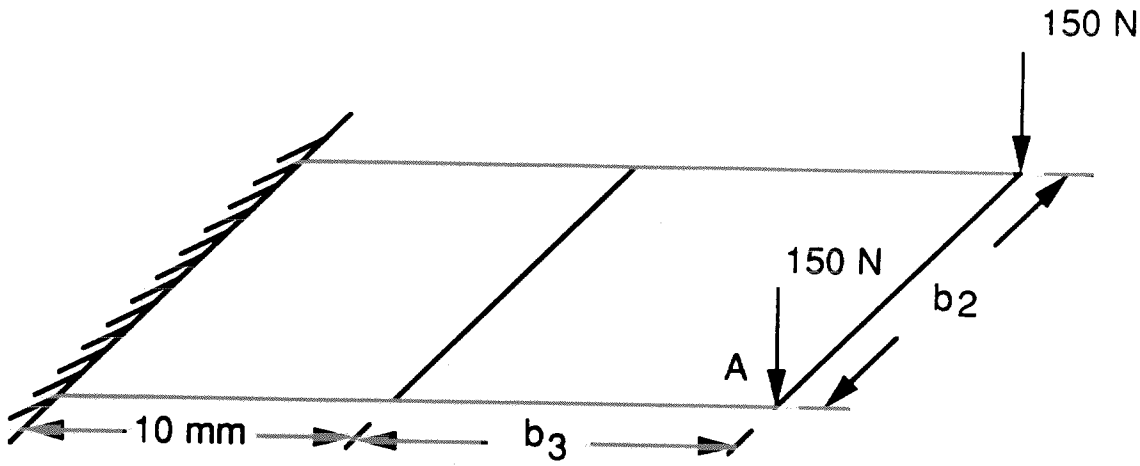

b_1 = thickness

Figure 7: Finite Element and Design Model of Cantilever Plate

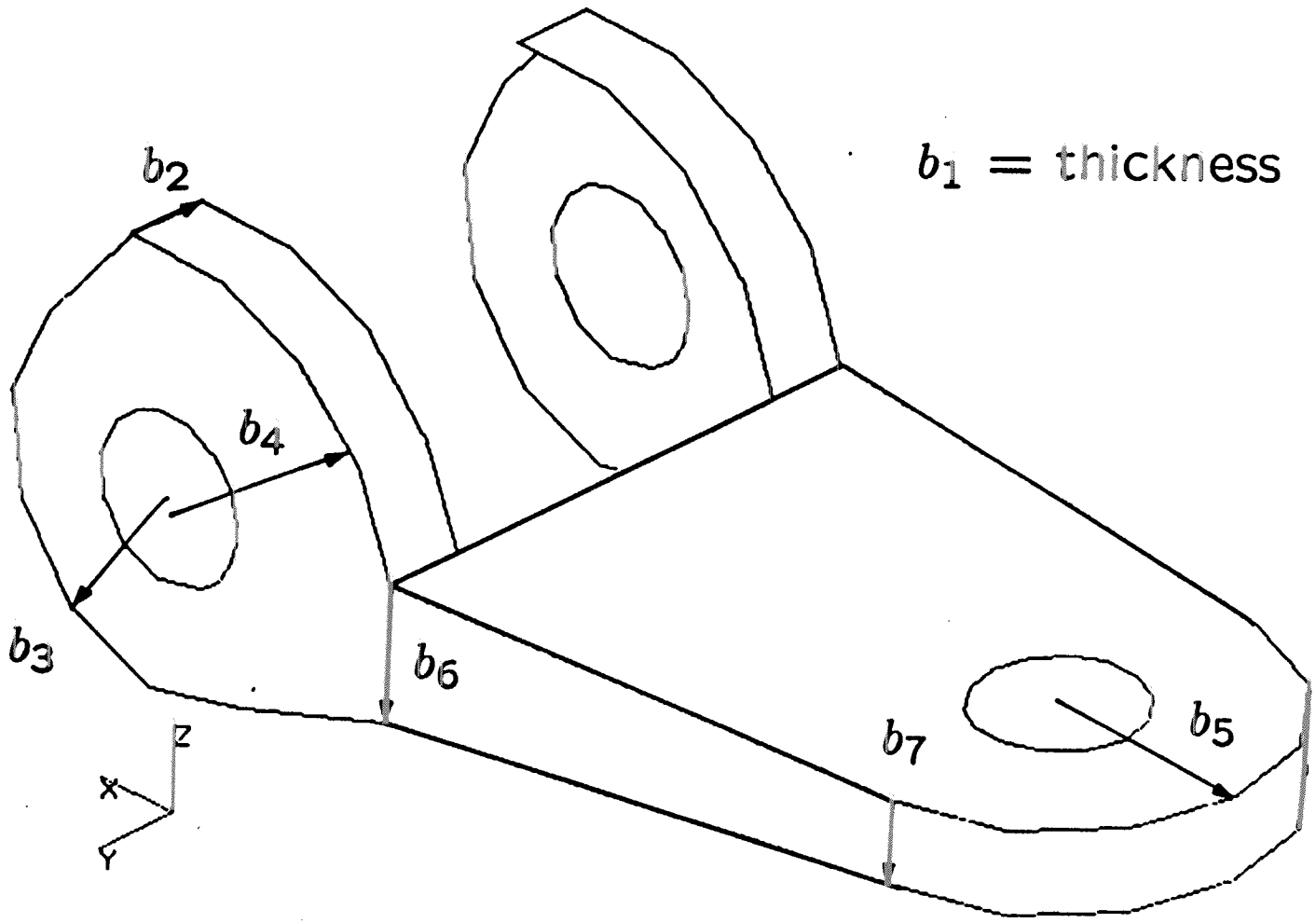

Figure 8: Design Model of Control Arm

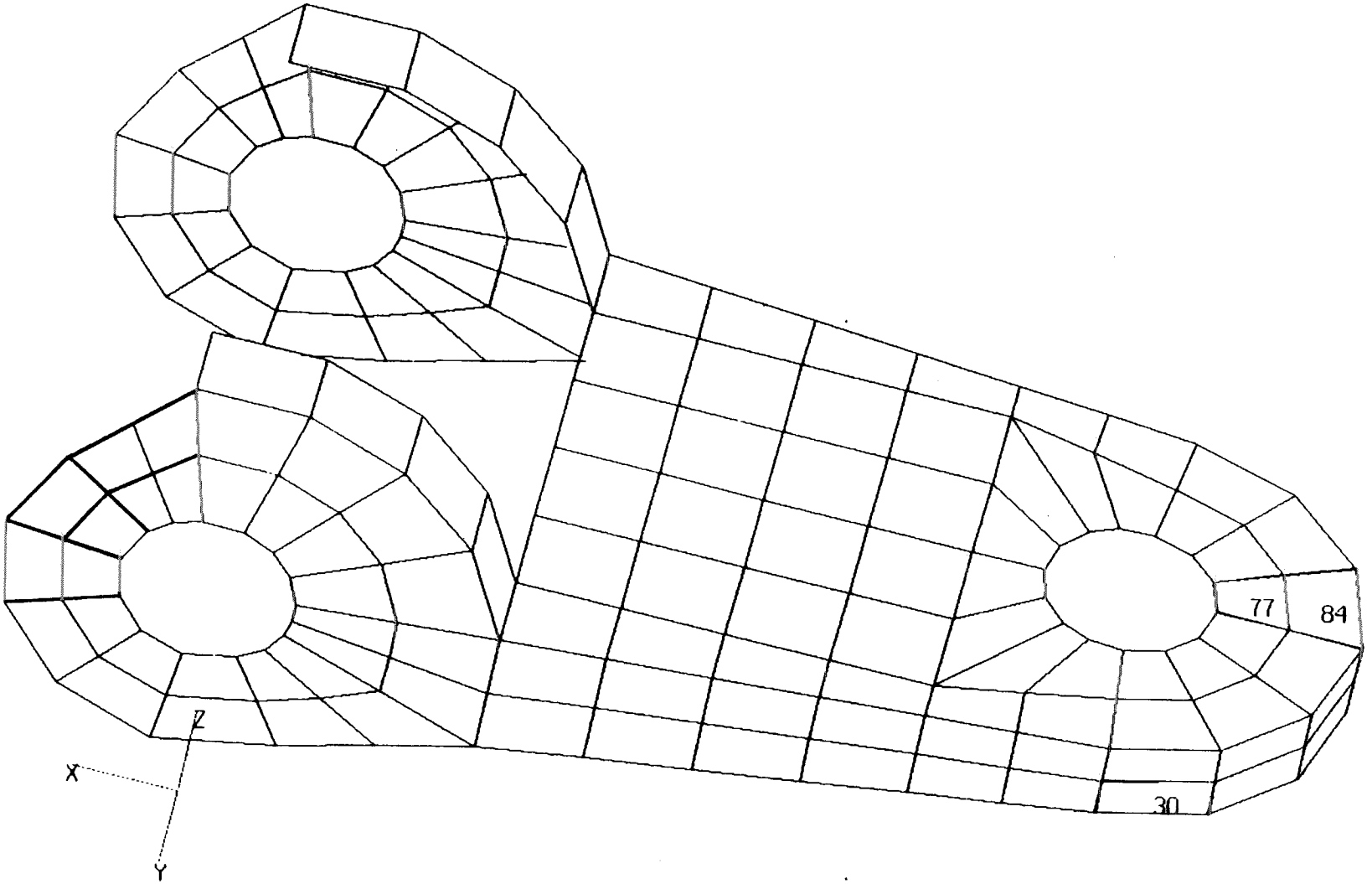

FIGURE 9: FINITE ELEMENT MESH OF CONTROL ARM

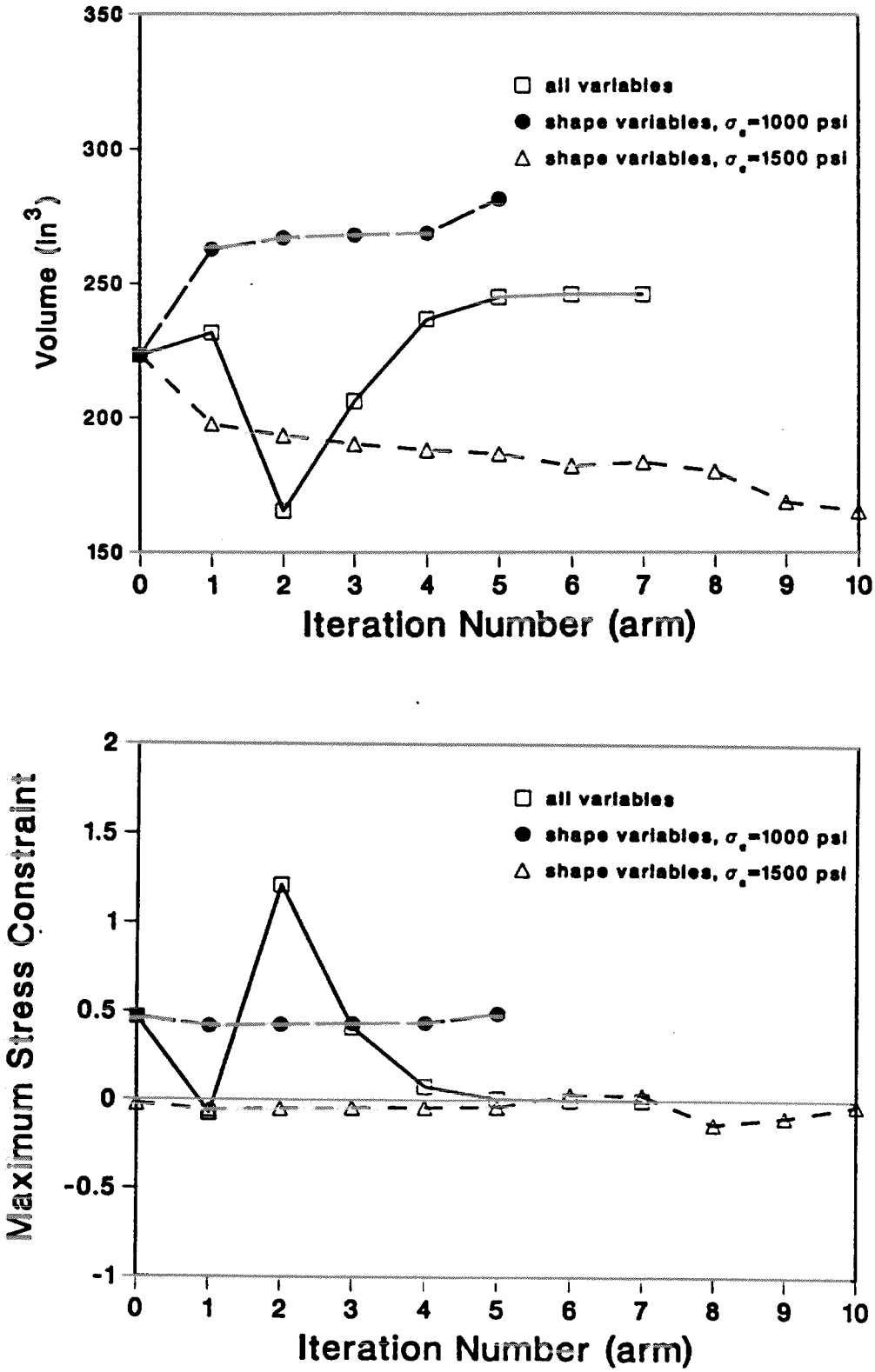

Figure 10: Design Histories of Control Arm